Korean J. Chem. Eng., **31**(10), 1746-1756 (2014)
DOI: 10.1007/s11814-014-0126-z

pISSN: 0256-1115
eISSN: 1975-7220

A comparative study of hybrid models combining various kinetic and regression models for *p*-xylene oxidation

Yaming Dong and Xuefeng Yan†

Key Laboratory of Advanced Control and Optimization for Chemical Processes of Ministry of Education, East China University of Science and Technology, Shanghai 200237, P. R. China
(*Received 18 November 2013 • accepted 29 April 2014*)

Abstract−The hybrid modeling approach, which combines kinetic and regression module parts to an overall process model, is an attractive process modeling approach. However, the selection of various kinetic and regression models affects the hybrid model performance. As an illustrating example, we investigated the *p*-xylene (PX) oxidation process and summarized the published results of the PX oxidation kinetic model. The kinetic parameters of three kinetic models (i.e., three frequently used kinetic models of PX oxidation) were estimated and the fitting results were evaluated. Six hybrid models were then developed based on these three kinetic models and two regression models (artificial neural network and support vector regression). Afterwards, a comparative study of the six hybrid models was carried out based on various kinetic and regression models. The performances of these kinetic and regression models on the hybrid models were also evaluated. Finally, the best suitable hybrid model was obtained for the PX oxidation process.

Keywords: Regression Model, Kinetic Model, Hybrid Model, *p*-Xylene Oxidation, Process Kinetics

INTRODUCTION

Process models are important because they can be used for various fields of process system engineering, such as process design, simulation, control, optimization and monitoring. The two common process model development approaches are the kinetic and the regression models.

Kinetic models (also known as first principle models), based on the fundamental conservation laws, are widely used in chemical processes [1]. Kinetic models use a set of mathematical equations to represent process behaviors [2]. A certain degree of extrapolation beyond the domain of the known process operating conditions is one of the greatest strengths of these models. However, the application of a kinetic model becomes restricted when partial knowledge about the physical phenomena taking place in the process is lacking. A common practice is to obtain the unknown parameters for the given operating conditions with data fitting techniques, so the different kinetic parameters will be obtained under this given experiment operating conditions. However, the real operating conditions are unpredictable so that the given experiments cannot cover them all. Thus the obtained kinetic parameters will become unsuitable for the unknown operating conditions.

The alternative process model development approaches are the regression approaches, which are directly identified from the existing plant measurement data without considering the process internal mechanism [3]. Such regression models are fitted to the real data according to a minimization criterion related to a norm of the differences (i.e., residuals) between estimates and observations [4]. The most commonly used regression approaches in the chemical processes are the artificial neural networks (ANN) [5-7] and the support vector regression (SVR) [8-12] because of their capability to accurately model the nonlinear and multi-dimensional processes [13,14]. However, the reliable predictions of the regression models highly depend on the adequate measurement data, and the predictions of such models are valid only inside the training data domain.

Psichogios et al. proposed the hybrid modeling approach, which combines the kinetic and regression module parts to an overall hybrid process model [15]. Compared with the kinetic model development, the hybrid modeling approach is faster and easier to apply. Furthermore, the extrapolation of the hybrid model is beyond the training data domain because it utilizes the kinetic model parts as the basis of the overall model. The successful application of the hybrid model in chemical and biochemical processes has been demonstrated [15-29]. Among these researches, most of the hybrid models used ANN as the regression model parts [15-24]. However, SVR and other regression methods are also used in the hybrid models [25-29].

Several kinetic models and a great number of regression models are available for one given chemical process. For the *p*-xylene (PX) oxidation process, three kinetic models were proposed in the literature [30-32]. Yan et al. [33,34] developed two regression models for the PX oxidation process. One is based on modified back propagation algorithm embedded with ridge regression, and the other is based on back propagation partial least square regression. However, how to choose these kinetic and regression models for the PX oxidation is a difficult task. In this paper, the published results of the PX oxidation kinetic model are summarized and the kinetic parameters of them estimated. Then, the three kinetic models and two typical regression models (ANN and SVR) are applied as various module parts for the development of PX oxidation hybrid model. The performance of the various combinations of module parts is evaluated. Finally, the best suited hybrid model of PX oxidation is obtained through a comparative study of the various kinds of hybrid models.

†To whom correspondence should be addressed.
E-mail: xfyan@ecust.edu.cn

This article is organized as follows. In section 2, the three kinetic models of PX oxidation are summarized, and the unknown parameters of these three kinetic models are estimated. Six hybrid models of PX oxidation combining three kinetic models with two regression models are developed in Section 3. The evaluation and comparative study of the three kinetic models, two regression models, and six hybrid models are included in Section 4. Finally, a brief conclusion is given in Section 5.

THREE KINETIC MODELS OF PX OXIDATION

1. Process Description

The direct oxidation of PX with air or molecular oxygen is a commercially important reaction for the production of terephthalic acid (TA), an important aromatic compound widely used in the polyester industry [31]. The oxidation of PX to TA occurs in acetic acid (HAC) solvent at the temperature range of 180 °C to 195 °C, catalyzed by cobalt and manganese acetate [$Co(Ac)_2$ and $Mn(Ac)_2$], and promoted by hydrogen bromide (HBr). These reactions involve several intermediates: *p*-tolualdehyde (TALD), *p*-toluic acid (TA), and 4-carboxybenzaldehyde (4-CBA). The lumped kinetic scheme for the oxidation of PX to TA is shown in Fig. 1 [31].

2. Kinetic Models

The liquid-phase oxidation of PX to TA is a typical free radical chain reaction that involves a very large number of radicals and molecular species [32]. Thus, its reaction mechanism has been extensively studied [30-32,35-37] because of its significant economic impact.

Cao and Cincotti investigated the kinetic process at low temperature of 80 °C to 130 °C, and proposed the kinetic model, assuming that all of the reactions were zeroth-order with respect to gaseous reactants and first-order to the liquid reactants [30,35-37]. Yan et al. then improved this model at a high temperature of 180 °C to 195 °C and assumed that all of the reactions were 0.65th-order with respect to PX and first-order to other liquid reactants [38]. The following population equations including four parameters are given as the lumped kinetic model:

$$\frac{dC_1}{dt} = -k_1^{cao} C_1^{n_1} C_{O_2}^{m_1} \tag{1}$$

$$\frac{dC_2}{dt} = k_1^{cao} C_1^{n_1} C_{O_2}^{m_1} - k_2^{cao} C_2^{n_2} C_{O_2}^{m_2} \tag{2}$$

$$\frac{dC_3}{dt} = k_2^{cao} C_2^{n_2} C_{O_2}^{m_2} - k_3^{cao} C_3^{n_3} C_{O_2}^{m_3} \tag{3}$$

$$\frac{dC_4}{dt} = k_3^{cao} C_3^{n_3} C_{O_2}^{m_3} - k_4^{cao} C_4^{n_4} C_{O_2}^{m_4} \tag{4}$$

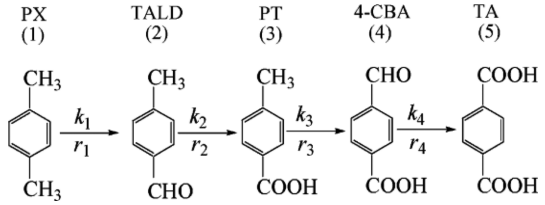

Fig. 1. Lumped kinetic scheme for the oxidation of *p*-xylene to terephthalic acid [31].

$$\frac{dC_5}{dt} = k_4^{cao} C_4^{n_4} C_{O_2}^{m_4} \tag{5}$$

Based on the complicated free radical chain-reaction mechanism, Wang et al. proposed a fractional kinetic model including 13 parameters shown in the following equations [31]:

$$\frac{dC_1}{dt} = -\frac{k_1^{wang} C_1}{\left(\sum_{i=1}^{4} d_i C_i + \theta\right)^{\beta_1}} \tag{6}$$

$$\frac{dC_2}{dt} = \frac{k_1^{wang} C_1}{\left(\sum_{i=1}^{4} d_i C_i + \theta\right)^{\beta_1}} - \frac{k_2^{wang} C_2}{\left(\sum_{i=1}^{4} d_i C_i + \theta\right)^{\beta_2}} \tag{7}$$

$$\frac{dC_3}{dt} = \frac{k_2^{wang} C_2}{\left(\sum_{i=1}^{4} d_i C_i + \theta\right)^{\beta_2}} - \frac{k_3^{wang} C_3}{\left(\sum_{i=1}^{4} d_i C_i + \theta\right)^{\beta_3}} \tag{8}$$

$$\frac{dC_4}{dt} = \frac{k_3^{wang} C_3}{\left(\sum_{i=1}^{4} d_i C_i + \theta\right)^{\beta_3}} - \frac{k_4^{wang} C_4}{\left(\sum_{i=1}^{4} d_i C_i + \theta\right)^{\beta_4}} \tag{9}$$

$$\frac{dC_5}{dt} = \frac{k_4^{wang} C_4}{\left(\sum_{i=1}^{4} d_i C_i + \theta\right)^{\beta_4}} \tag{10}$$

Later, Sun et al. developed a simplified free radical kinetic model for PX oxidation [32] that considers the concentrations of various kinds of peroxy free radical, including six parameters shown in Eqs. (11) to (21):

$$\frac{dC_1}{dt} = -k_1^{sun} C_1 - k_2^{sun} C_2 \tag{11}$$

$$\frac{dC_2}{dt} = MC_{[O]_1} - k_1^{sun} C_2 - k_3^{sun} C_{[O]} C_2 \tag{12}$$

$$\frac{dC_3}{dt} = MC_{[O]_2} - k_1^{sun} C_3 - k_4^{sun} C_{[O]} C_3 \tag{13}$$

$$\frac{dC_4}{dt} = MC_{[O]_3} - k_1^{sun} C_4 - k_5^{sun} C_{[O]} C_4 \tag{14}$$

$$\frac{dC_5}{dt} = MC_{[O]_4} \tag{15}$$

$$\frac{dC_{[O]_1}}{dt} = k_1^{sun} C_1 + k_2^{sun} C_{[O]} C_1 - CC_{[O]_1} - k_6^{sun} C_{[O]_1} (C_{[O]} + C_{[O]_1}) \tag{16}$$

$$\frac{dC_{[O]_2}}{dt} = k_1^{sun} C_2 + k_3^{sun} C_{[O]} C_2 - CC_{[O]_2} - k_6^{sun} C_{[O]_2} (C_{[O]} + C_{[O]_2}) \tag{17}$$

$$\frac{dC_{[O]_3}}{dt} = k_1^{sun} C_3 + k_4^{sun} C_{[O]} C_3 - CC_{[O]_3} - k_6^{sun} C_{[O]_3} (C_{[O]} + C_{[O]_3}) \tag{18}$$

$$\frac{dC_{[O]_4}}{dt} = k_1^{sun} C_4 + k_5^{sun} C_{[O]} C_4 - CC_{[O]_4} - k_6^{sun} C_{[O]_4} (C_{[O]} + C_{[O]_4}) \tag{19}$$

$$C_{[O]} = C_{[O]_1} + C_{[O]_2} + C_{[O]_3} + C_{[O]_4} \tag{20}$$

$$M = k_2^{sun} C_1 + k_3^{sun} C_2 + k_4^{sun} C_3 + k_5^{sun} C_4 \tag{21}$$

Table 1. Parameters of three kinetic models for PX oxidation

Researchers	Parameters
Cao et al. and Yan et al. [30,38]	4 Variable kinetic parameters, i.e. k_1^{cao}, k_2^{cao}, k_3^{cao}, k_4^{cao}, with changing operating conditions.
Wang et al. [31]	4 Variable kinetic parameters, i.e. k_1^{wang}, k_2^{wang}, k_3^{wang}, k_4^{wang}, and 9 constant parameters, i.e. d_i, θ, β_i (i=1, …, 4).
Sun et al. [32]	1 Variable kinetic parameters, i.e. k_1^{sun}, and 5 constant parameters, i.e., k_2^{sun}, k_3^{sun}, k_4^{sun}, k_5^{sun}, k_6^{sun}

These three kinetic models have been frequently used in PX oxidation [18,38-41]. The model parameters are listed in Table 1.

3. Parameter Estimation

When the model framework is determined, parameter estimation is an essential step in the development of the kinetic model. To compare the performance of the three kinetic models under the same conditions, their parameters were re-estimated using the same experimental data obtained from the work of Wang [31]. Considering that variable parameters and constant parameters are available with the changing operating conditions in the three kinetic models, a two-step parameter estimation method proposed in a previous paper [42] was used to determine the variable and constant parameters.

The two-step method for kinetic parameter estimation is a kind of decomposition coordination strategy that the optimization goal was decomposed into two steps goals. At the first step, the variable parameters (i.e., k_i^{cao}, k_i^{wang}, k_i^{sun}) are estimated by minimizing the difference between the simulated and the experimental time evolution of the product composition for the experimental runs for the given values of constant variable (i.e., d_i, θ, β_i, k_{2-6}^{sun}); at the second step, the values of constant variables are estimated by minimizing the average difference of experimental runs at the first step. There are iterations between two steps until the convergence. And the Sim-

Table 2. Obtained kinetic parameters for the kinetic model of Cao with 95% confidence intervals

Run	k_1^{cao}	k_2^{cao}	k_3^{cao}	k_4^{cao}
Run1	0.1631±0.0118	0.6030±0.1702	0.0499±0.0042	0.4803±0.2749
Run2	0.2231±0.0178	0.7224±0.1793	0.0720±0.0065	0.5938±0.3089
Run3	0.2873±0.0169	1.0291±0.1400	0.1490±0.0098	0.9803±0.3269
Run4	0.4687±0.0559	1.6753±0.4262	0.2915±0.0362	2.0147±1.3053
Run8	0.2658±0.0197	0.8270±0.1414	0.1089±0.0082	0.7732±0.2913
Run9	0.3312±0.0276	0.9308±0.1799	0.1320±0.0115	0.9713±0.4487
Run10	0.4081±0.0297	1.0661±0.1624	0.1476±0.0105	1.0434±0.3639
Run11	0.4245±0.0318	1.2788±0.2377	0.1972±0.0182	1.4328±0.6768
Run12	0.2346±0.0174	0.7357±0.1321	0.0977±0.0079	0.7027±0.3119
Run13	0.4525±0.0326	1.2004±0.1844	0.1790±0.0127	1.1486±0.3967
Run14	0.4878±0.0479	1.1849±0.2485	0.2324±0.0269	1.4443±0.7547
Run15	0.2346±0.0155	0.6948±0.1103	0.0893±0.0059	0.6163±0.2000
Run16	0.3937±0.0407	1.0546±0.2397	0.1720±0.0195	1.2085±0.7052
Run17	0.4552±0.0401	1.0931±0.1980	0.2202±0.0213	1.4373±0.6788

Table 3. Obtained variable kinetic parameters for the kinetic model of Wang with 95% confidence intervals

Run	k_1^{wang}	k_2^{wang}	k_3^{wang}	k_4^{wang}
Run1	0.8691±0.0257	1.6050±0.2121	0.1510±0.0099	0.9158±0.1766
Run2	0.8752±0.0228	1.4514±0.1445	0.1268±0.0072	0.8476±0.1323
Run3	0.7320±0.0307	1.4219±0.1799	0.1390±0.0119	0.8725±0.1323
Run4	0.7448±0.0529	1.3258±0.2695	0.1433±0.0203	1.2223±0.4815
Run8	0.6756±0.0306	1.0061±0.1428	0.0940±0.0083	0.6907±0.1599
Run9	0.8011±0.0455	1.0160±0.1793	0.1089±0.0130	0.7995±0.2451
Run10	0.9656±0.0370	1.1940±0.1355	0.1326±0.0100	0.9335±0.1760
Run11	1.0439±0.0653	1.5071±0.3060	0.1703±0.0237	1.2594±0.4645
Run12	0.5498±0.0314	0.9171±0.1720	0.0879±0.0107	0.6156±0.1914
Run13	1.0449±0.0553	1.4454±0.2341	0.1567±0.0166	0.9789±0.2384
Run14	1.1983±0.1068	1.2203±0.3182	0.1939±0.0377	1.2069±0.5229
Run15	0.5813±0.0258	0.8512±0.1223	0.0774±0.0064	0.5481±0.1147
Run16	0.9396±0.0366	1.2114±0.1429	0.1495±0.0129	1.0837±0.2411
Run17	1.0584±0.0416	1.2077±0.1390	0.1871±0.0162	1.2386±0.2535

Table 4. Obtained constant kinetic parameters for the kinetic model of Wang with 95% confidence intervals

i	d_i	β_i	θ
1	3.4004±0.1143	0*	0.0472±0.0338
2	−0.7642±0.3493	0.6111±0.0560	
3	1.0563±0.2051	0*	
4	3.7038±1.5227	0.7048±0.1419	

*: β_1 and β_3 were introduced by Wang et al. [31] and set to be zero directly because the oxidations of aldehydes have higher manifestation orders than the oxidations of hydrocarbon. Thus, in our trial, $\beta_1=\beta_3=0$ directly and are not re-estimated

Table 5. Obtained variable kinetic parameters for the kinetic model of Sun with 95% confidence intervals

Run	$k_1^{sun}\times10^7$
Run1	4.0951±0.3683
Run2	16.4046±1.4276
Run3	99.9425±7.5764
Run4	739.1660±48.1683
Run8	69.9807±5.8704
Run9	94.4736±8.4141
Run10	136.1121±8.6185
Run11	183.8193±19.5170
Run12	50.8358±4.9817
Run13	164.1232±16.0974
Run14	228.0402±30.7350
Run15	49.4511±4.3102
Run16	142.8701±8.8696
Run17	194.6393±19.8543

plex method, which is one of the most commonly used traditional optimization algorithm, was employed for the two-step method.

The obtained optimal parameters with 95% confidence intervals of these three kinetic models are listed in Tables 2 to 6. Considering that the influence of oxygen partial pressure (experimental runs 5-7) on PX oxidation can be neglected when the oxygen partial pressure does not drop below a minimum value, i.e., 0.2 bar, the experimental runs 5 to 7 are not considered in this paper [43,44].

HYBRID MODELS FOR PX OXIDATION

After the unknown parameters were obtained, the three kinetic models were developed. However, the application of these kinds of kinetic models is still limited when one looks for the prediction results on the different operating conditions. Given that the kinetic parameters were obtained from the direct fitting of the model results with the measurement data under given operating conditions, so the different kinetic parameters will be obtained under this given experiment operating conditions. However, the real operating conditions are unpredictable so that the given experiments cannot cover them all. Thus the obtained kinetic parameters become unsuitable for the unknown operating conditions. The main reasons of this issue are that the precise mathematical relationship between the kinetic parameters and various operating conditions is unknown.

The hybrid model, which combines kinetic model and regression model, provides a new idea for solving this problem. The regression model (ANN, SVR or other regression method) can be used to describe the relationship between the unknown kinetic parameters and the various operating conditions. The kinetic model representing the basic of the hybrid model is then used to predict the concentrations of the interesting materials.

For one given process, several kinetic models (three kinetic models for PX oxidation) and variety of regression models are available. The selection of this partial models in the development of hybrid model is important because it will make the unknown difference on the overall model performance. In this section, six hybrid models that combines three kinetic models (kinetic models of Cao, Wang and Sun) and two regression models (ANN and SVR) will be developed for PX oxidation.

1. Data Collection and Preprocessing

Among the parameters of the three kinetic models described in Section 2.2, the kinetic rate constants k_i are the most sensitive for the influence by many operating conditions, such as initial concentration of PX, temperature, catalyst, and bromide concentrations [18,31]. Considering that the precise mathematical model of the rate constants is unknown in the literature, the regression models will be used to develop the rate constant model.

Based on the known knowledge of the process kinetic, 14×5 experiment operating conditions collected from [31], in which 14 is the number of data sets and 5 is the number of input variables (i.e., reaction temperature (x_1, °C); initial concentration of PX (x_2, mol/kg acetic acid); concentration of cobalt catalyst in the feed (x_3, ppmw); concentration of manganese catalyst in the feed (x_4, ppmw); concentration of bromide promoter in the feed (x_5, ppmw)) were used as input data of the rate constant regression models. The obtained 14×4 (i.e., k_1^{cao}, k_2^{cao}, k_3^{cao}, k_4^{cao}), 14×4 (i.e., k_1^{wang}, k_2^{wang}, k_3^{wang}, k_4^{wang}), and 14×1 (i.e., k_1^{sun}) rate constants values were used as output data of the rate constant regression models for the kinetic models of Cao, Wang, and Sun, respectively. Afterward, three data sets, i.e., 14×9, 14×9, and 14×6, were obtained for the development of rate constant regression models. Before modeling, all the data sets were normalized to [0 1] by (x-min(x))/(max(x)-min(x)).

2. Regression Models for Kinetic Rate Constants

In the present study, the kinetic rate constants for the operating conditions (i.e., x_1, x_2, x_3, x_4, and x_5) were modeled using ANN and SVR.

As one of the most popular network structure for ANN, the three-layer back propagation neural network (BPNN) was used to predict the kinetic rate constants, and three BPNN models were developed for the three data sets separately. The number of neurons was selected on the principle of minimizing the training error and the

Table 6. Obtained constant kinetic parameters for the kinetic model of Sun with 95% confidence intervals

$k_2^{sun}\times10^{-4}$	$k_3^{sun}\times10^{-4}$	$k_4^{sun}\times10^{-3}$	$k_5^{sun}\times10^{-4}$	k_6^{sun}
2.4974±0.1002	4.2062±0.2983	2.3319±0.1670	1.6865±0.3057	0.5913±0.0183

MATLAB ANN toolbox was used in this paper.

Three SVR models were also developed for these three data sets. To develop a successful SVR model, several parameters, including the kernel type, loss function type, kernel parameters σ, and model parameters C and ε were evaluated. In this study, kernel type was chosen as the RBF function and the loss function type was the ε-insensitive loss function. C, σ, and ε were chosen on the principle of minimizing the training error. An SVR-implementation known as "ε-SVR" in the LIBSVM software library [45] was used.

Leave-one-out cross validation method was employed to ANN and SVR to verify the performance of these regression models. In

Table 7. Parameter values of the SVR models

Rate constant	C	σ	ε
k_1^{cao}	30	0.21	0.01
k_2^{cao}	40	0.22	0.01
k_3^{cao}	19	0.19	0.01
k_4^{cao}	50	0.01	0.01
k_1^{wang}	51	0.15	0.001
k_2^{wang}	25	0.3	0.12
k_3^{wang}	1	0.12	0.001
k_4^{wang}	25	0.01	0.001
k_1^{sun}	1	0.1	0.01

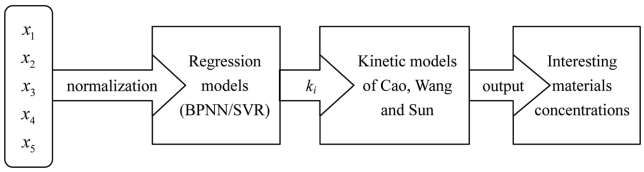

Fig. 2. Schematic of the hybrid models of PX oxidation.

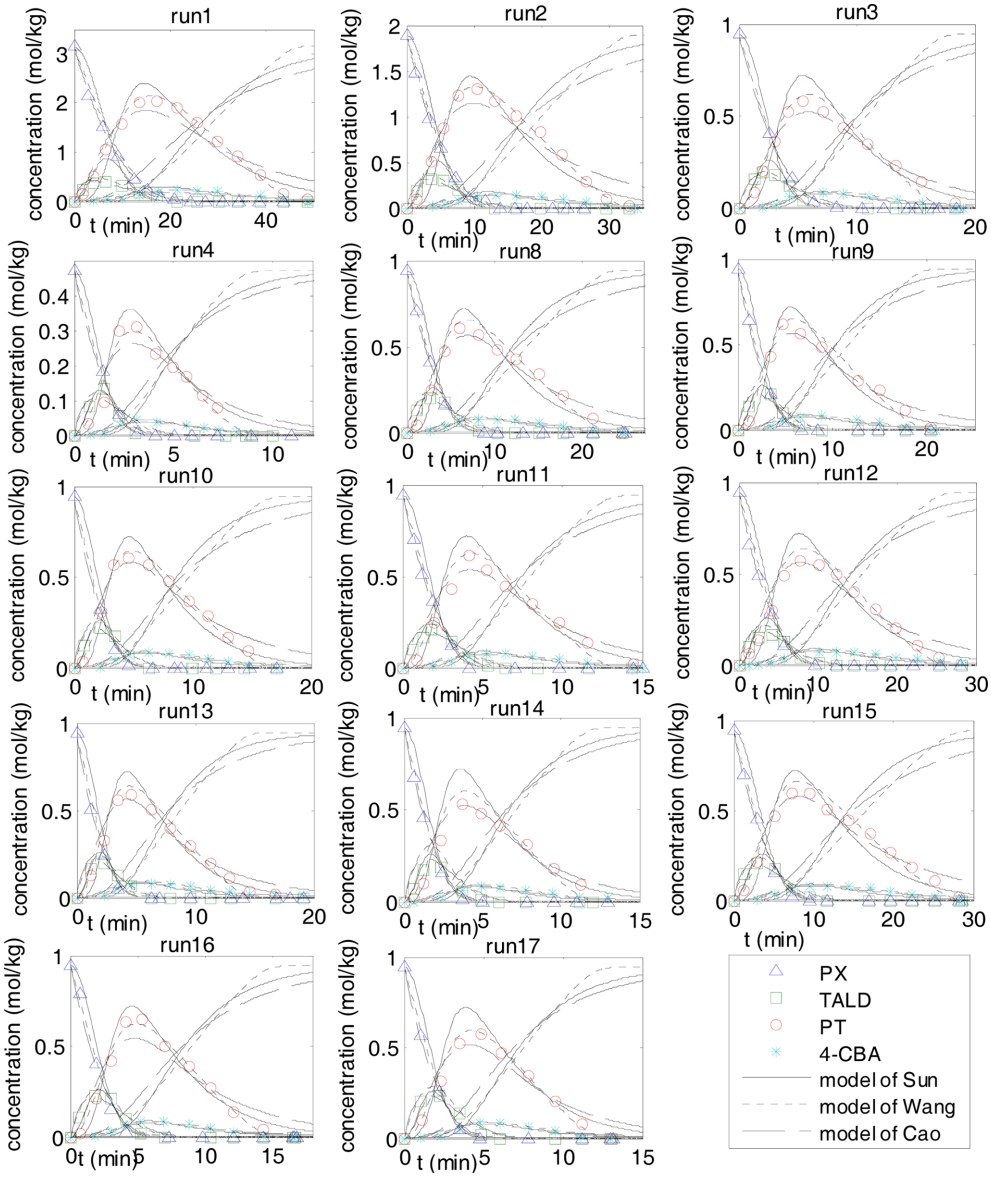

Fig. 3. Evolution of the experimental and simulated material concentrations for the kinetic models of Cao, Wang and Sun. The parameters in the kinetic models are from section 2.3, Tables 2 to 6.

each round, one of the experimental data was partitioned from the 14 experimental data to be the test data, and the other 13 data were the training data. The leave-one-out cross validation has 14 rounds, and each experimental data has 13 times as training data and 1 time as testing data. An average of the error corresponding to the left-one subsets, known as 'cross-validation error' gives an estimate of the model performance. After evaluation of the model for the wide range of model parameters (grid search methodology for SVR), the optimal values of model parameters were obtained. The values of SVR parameters C, σ, and ε are listed in Table 7.

3. Hybrid Process Models

After the regression models of the kinetic rate constants are developed, the predicted rate constants can be used for the kinetic models to calculate the concentrations of the interesting materials as a function of time. The schematic of the hybrid models is shown in Fig. 2.

RESULTS AND DISCUSSION

The following model evaluation parameters were used for the statistical analyses of the above kinetic models, regression models, and hybrid models:

1. The root mean square error (RMSE) used to evaluate the model should be minimum and was given by

$$\mathrm{RMSE}=\sqrt{\frac{\sum_{i=1}^{N}(y_{exp}-y_{pred})^2}{N}} \tag{22}$$

Table 8. Fitting evaluation results of the three kinetic models

Kinetic model	RMSE	MAE	CC
Kinetic model of Cao	0.0315	0.0230	0.9667
Kinetic model of Wang	0.0239	0.0165	0.9902
Kinetic model of Sun	0.0471	0.0302	0.9736

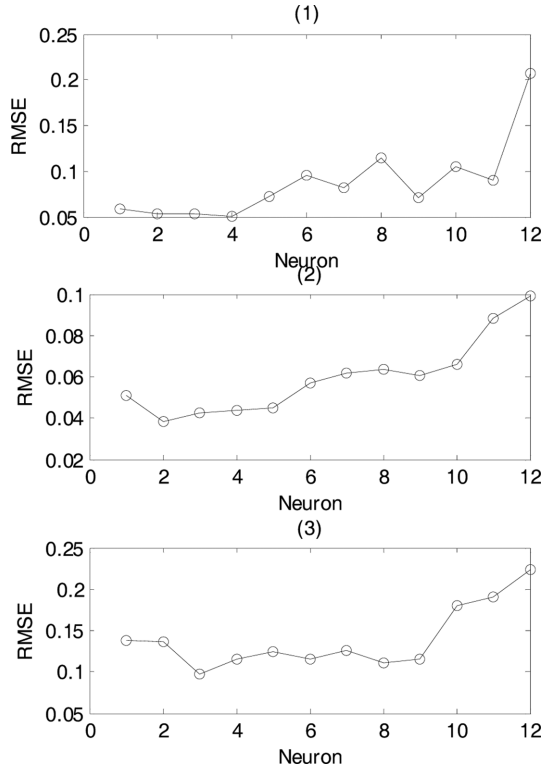

Fig. 4. Relationships between hybrid models prediction RMSE and the number of network hidden neurons.

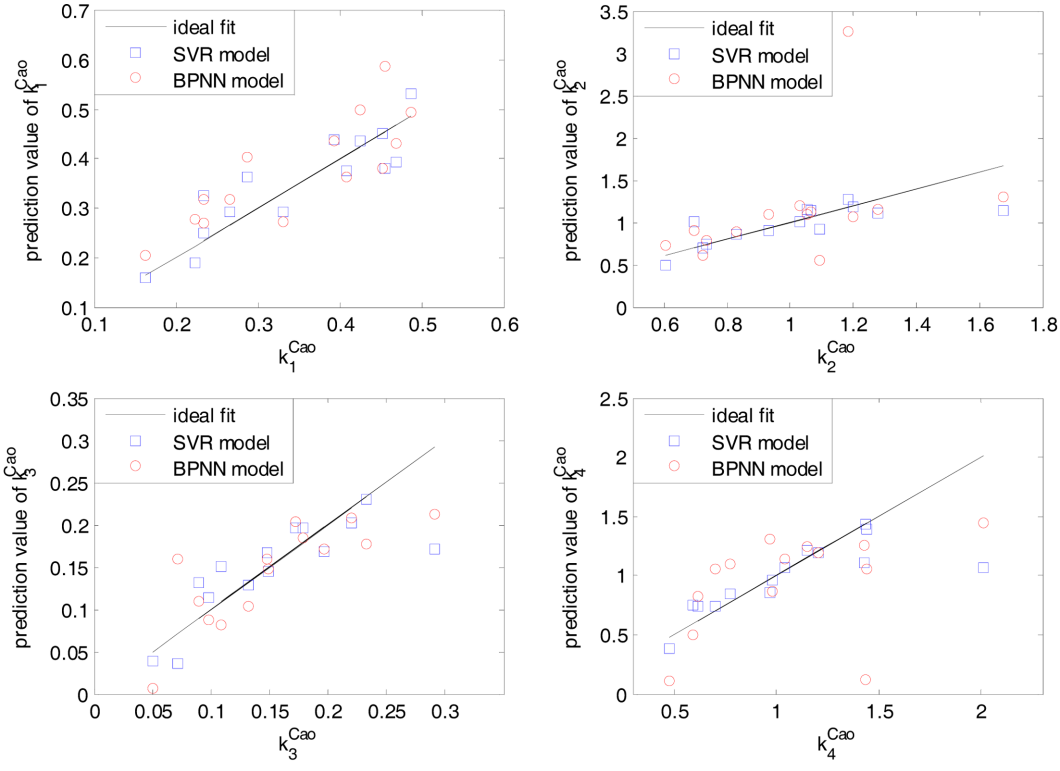

Fig. 5. Prediction results of the rate constant regression models for the kinetic model of Cao.

2. The mean absolute error (MAE) should be minimum, calculated as follows:

$$MAE = \frac{\sum_{i=1}^{N} |y_{exp} - y_{pred}|}{N} \quad (23)$$

3. The correlation coefficient (CC) for evaluating the model should be maximum

$$CC = \frac{\sum_{i=1}^{N} (y_{exp} - y_{exp(mean)})(y_{pred} - y_{pred(mean)})}{\sqrt{\sum_{i=1}^{N} (y_{exp} - y_{exp(mean)})^2} \sqrt{\sum_{i=1}^{N} (y_{pred} - y_{pred(mean)})^2}} \quad (24)$$

where y_{exp} denotes the experimental data; $y_{exp(mean)}$ denotes the mean value of y_{exp}; y_{pred} denotes the prediction value of output; and $y_{pred(mean)}$ denotes the mean value of y_{pred}.

1. Fitting Results of the Kinetic Models

The time evolution of the experimental material concentrations, along with the simulated values for the kinetic models of Cao, Wang, and Sun, is summarized in Fig. 3. The kinetic parameters used in these models were from Section 2.3, Tables 2 to 6. The fitting evaluation results of these three kinetic models are shown in Table 8. The results showed that the fitting results of the kinetic model of Wang were the best in this three kinetic models, whereas the model of Sun was the worst. From Table 8 we can see that the RMSE and MAE of these three models are small, and the correlation coefficient (CC) is larger than 95%, so they all have satisfying fitting performance.

2. Prediction Results of the Hybrid Models

The relationships between the hybrid model prediction RMSE and the number of network hidden neurons are shown in Fig. 4, in which, Fig. 4(1-3) are the results of the BPNN rate constant based hybrid models based on the kinetic models of Cao, Wang, and Sun, respectively. Fig. 4 shows that the numbers of network hidden neurons were chosen as 4, 2, and 3, respectively, because the hybrid models have the best predicting ability at these points.

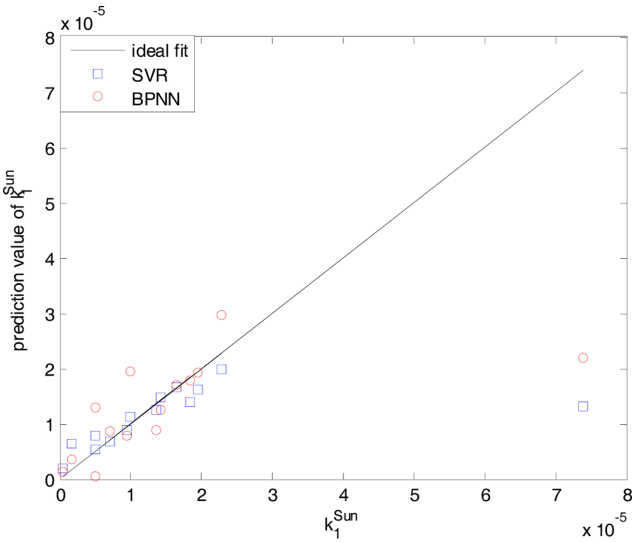

Fig. 7. Prediction results of the rate constant regression models for the kinetic model of Sun.

A comparison between the values of the kinetic rate constants (k_i^{Cao}: kinetic rate constants for the kinetic model of Cao; k_i^{Wang}: kinetic rate constants for the kinetic model of Wang; k_i^{Sun}: kinetic rate constant for the kinetic model of Sun) predicted by the kinetic models of BPNN and SVR with those of the data from Tables 2, 3, and 5 are

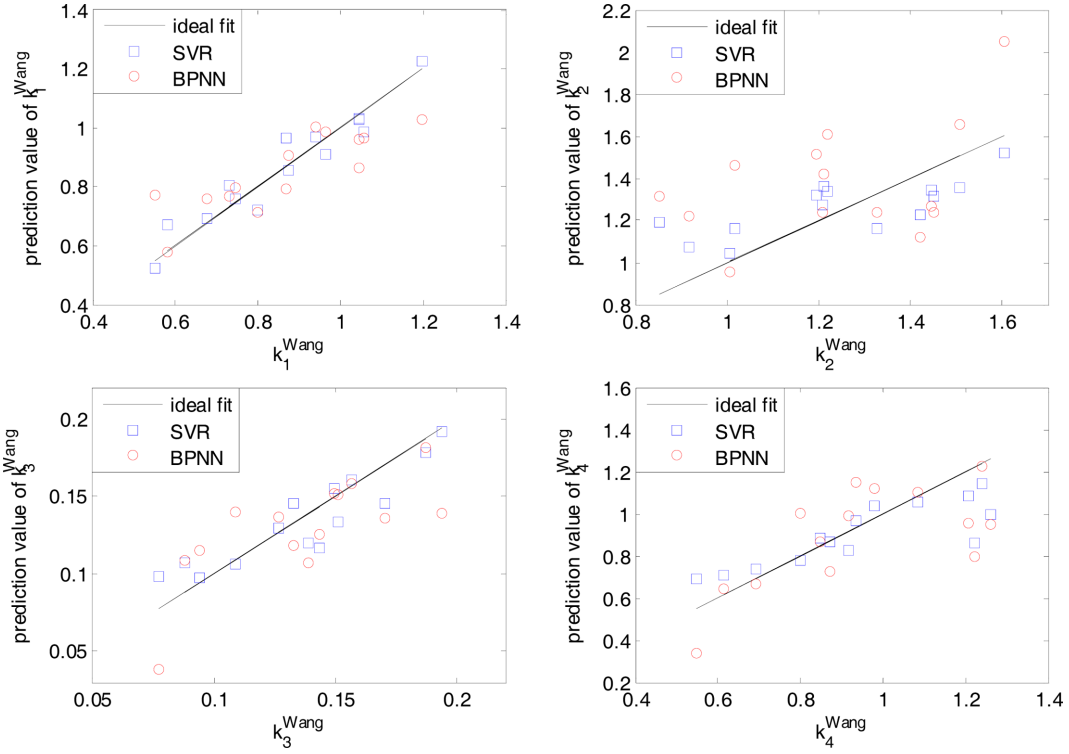

Fig. 6. Prediction results of the rate constant regression models for the kinetic model of Wang.

Table 9. Training and prediction errors of the rate constants regression models for the kinetic model of Cao

Model	k_1^{Cao}		k_2^{Cao}		k_3^{Cao}		k_4^{Cao}	
	RMSE	MAE	RMSE	MAE	RMSE	MAE	RMSE	MAE
BPNN	0.0597/0.0605	0.0394/0.0444	0.1071/0.2871	0.0659/0.2302	0.0326/0.0549	0.0232/0.0375	0.1836/0.3981	0.1203/0.2844
SVR	0.0215/0.0490	0.0152/0.0404	0.1207/0.1857	0.0507/0.1213	0.0236/0.0396	0.0143/0.0275	0.2644/0.2780	0.1231/0.1465

Table 10. Training and prediction errors of the rate constants regression models for the kinetic model of Wang

Model	k_1^{Wang}		k_2^{Wang}		k_3^{Wang}		k_4^{Wang}	
	RMSE	MAE	RMSE	MAE	RMSE	MAE	RMSE	MAE
BPNN	0.1206/0.1056	0.0883/0.0859	0.1827/0.2921	0.1309/0.2554	0.0235/0.0256	0.0189/0.0202	0.1300/0.1921	0.0936/0.1480
SVR	0.0321/0.0543	0.0167/0.0452	0.1168/0.1569	0.1118/0.1415	0.0095/0.0149	0.0062/0.0121	0.1233/0.1386	0.0715/0.1000

Table 11. Training and prediction errors of the rate constant regression models for the kinetic model of Sun

Model	k_1^{Sun}	
	RMSE	MAE
BPNN	1.10e-5/1.46e-5	5.71e-6/6.78e-6
SVR	1.58e-5/1.64e-5	5.47e-6/6.05e-6

shown in Figs. 5 to 7. The training and prediction errors of BPNN and SVR are shown in Tables 9 to 11, in which the values in the left of the slash are the training errors, whereas the right ones are the prediction errors. The SVR-based rate constant model has a better training and prediction performance than BPNN. One possible reason for this result is that SVR has better ability for modeling the highly nonlinear relationships based on the small sample than BPNN.

The prediction results of the various hybrid models for the interesting material concentrations are shown in Figs. 8 to 10, and the prediction error of these hybrids models is listed in Table 12, in which, BPNN+Cao, BPNN+Wang, and BPNN+Sun indicate that the hybrid models combine the rate constant regression models of BPNN with the kinetic models of Cao, Wang, and Sun, respectively. Meanwhile, SVR+Cao, SVR+Wang, and SVR+Sun indicate that the hybrid models combine the rate constant regression models of SVR with the kinetic models of Cao, Wang, and Sun, respectively.

These results show that the prediction performance of the hybrid models based on the kinetic model of Wang is better than those of Cao and Sun. The reasons for these results are that the fitting results of the kinetic model of Wang were the best and the prediction performance of the rate constant regression models for the kinetic model of Wang was also satisfactory. Although the prediction performance of the rate constant regression models for the kinetic model of Cao was better than that of Wang, the intrinsic drawbacks of the kinetic

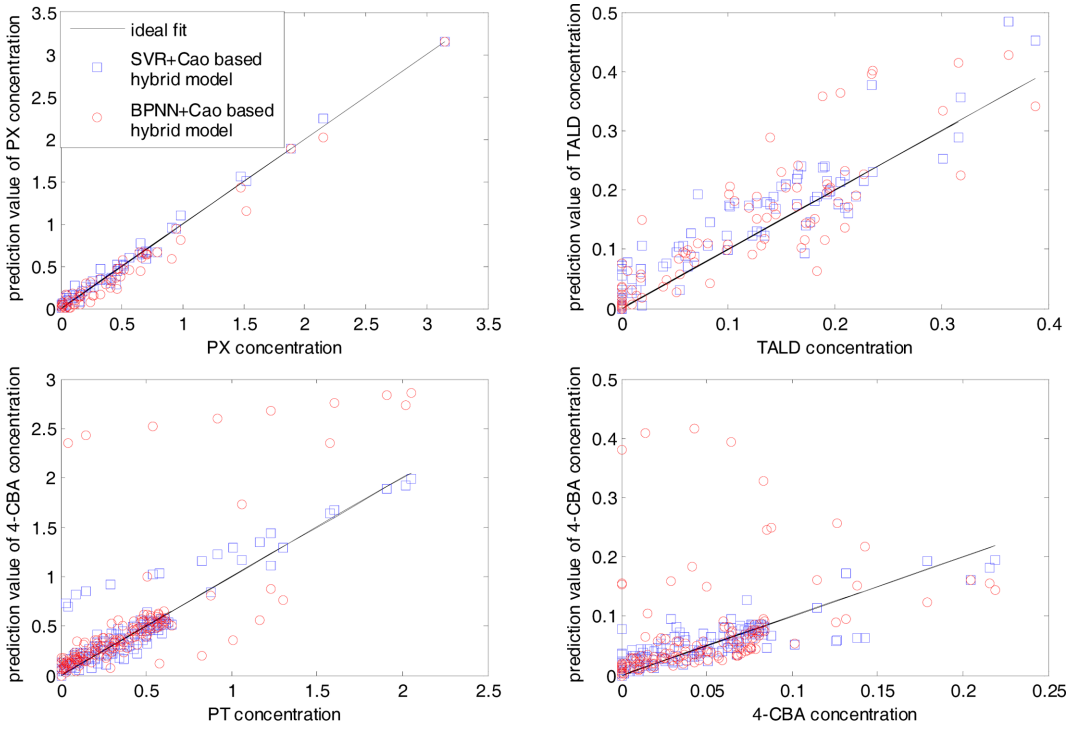

Fig. 8. Prediction results of the hybrid models based on the kinetic model of Cao.

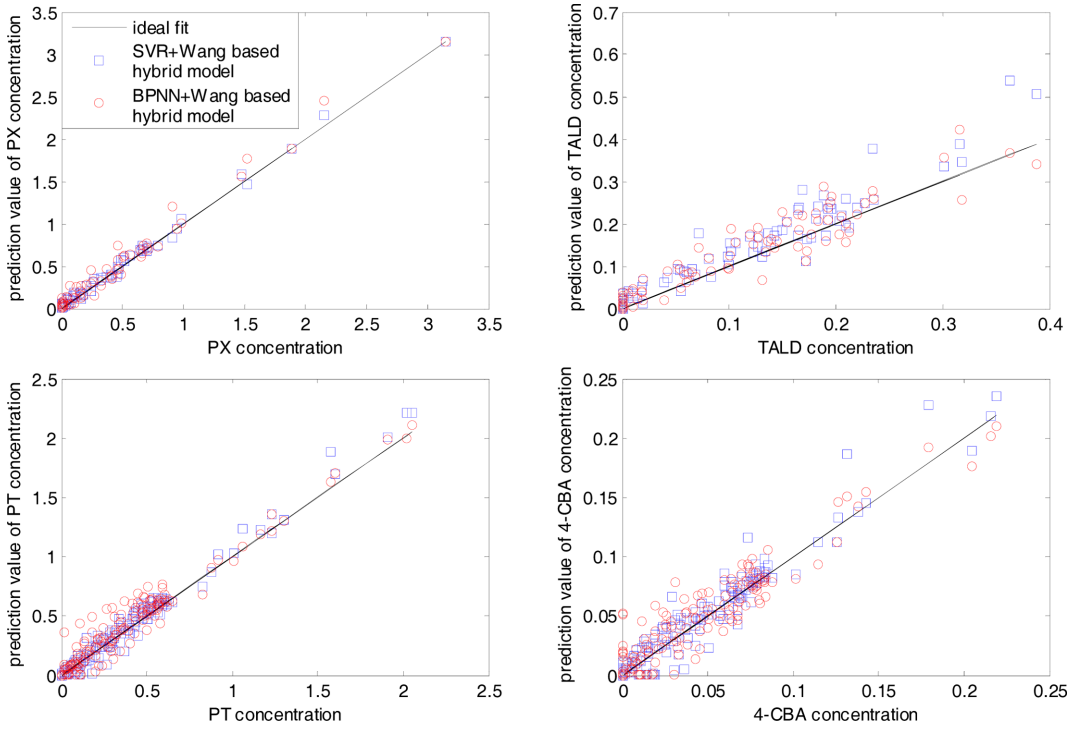

Fig. 9. Prediction results of the hybrid models based on the kinetic model of Wang.

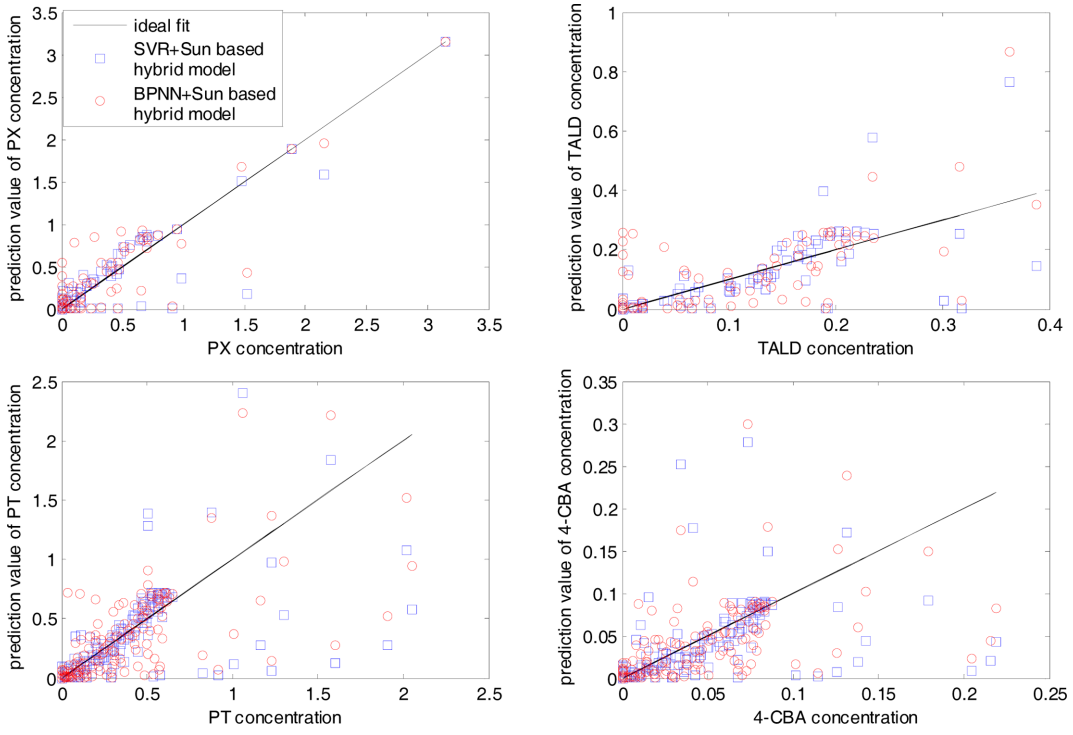

Fig. 10. Prediction results of the hybrid models based on the kinetic model of Sun.

model of Cao (i.e., the kinetic model did not consider the detailed reaction mechanism of PX oxidation [32], and the kinetics previously obtained by Cao is empirical and did not reveal the reaction mechanism sufficiently [31]), causing the performance of the SVR+Cao based hybrid model to be poorer than the SVR+Wang based hybrid model. The performance of the hybrid models based on the kinetic model of Sun was the worst in these six hybrid models. Thus, in the development of the hybrid model, we should choose the kinetic model whose unknown parameters are easier to model and has fewer fitting errors.

Table 12. Prediction errors of the six kinds of hybrid models

Hybrid model	RMSE	MAE	CC
BPNN+Cao	0.0509	0.0372	0.9197
SVR+Cao	0.0485	0.0344	0.9372
BPNN+Wang	0.0408	0.0294	0.9642
SVR+Wang	0.0307	0.0216	0.9820
BPNN+Sun	0.0976	0.0689	0.7980
SVR+Sun	0.0887	0.0612	0.8533

For these six hybrid models, the performances of SVR based hybrid models are better than that of the BPNN based ones. Considering that the sample data used for the rate constant regression model is too small, the performance of BPNN is not fully shown. Thus, SVR is a better choice in the case of small experimental data when one wants to develop a hybrid model for the chemical process.

Tables 8 and 12 show that the prediction performance of the SVR+Wang based hybrid model is close to the fitting results of the kinetic model of Wang, and the correlation coefficient 0.9820 is also satisfactory. Thus, the SVR+Wang based hybrid model is the best suitable hybrid model for PX oxidation, and can be used for process optimization under various operating conditions.

CONCLUSIONS

The published results of PX oxidation kinetic model have been summarized. The kinetic parameters of three kinetic models (i.e., three frequently used kinetic models of PX oxidation) were estimated by a two-step parameter estimation method and the fitting results were evaluated indicating that the kinetic model of Wang was the best. Six hybrid models were then developed based on these three kinetic models and two regression models (i.e., artificial neural network and support vector regression) for the PX oxidation process.

A comparative study of the six hybrid models was carried out based on various kinetic and regression models. The role of various kinetic and regression models on the performance of hybrid model was evaluated because these two factors have an important effect on the performance of the hybrid model. The prediction performance of the hybrid models based on the kinetic model of Wang is better than those of Cao and Sun. Results show that in the development of the hybrid model, we should choose the kinetic model whose unknown parameters are easier to model and has fewer fitting errors.

For the six hybrid models, the performance of SVR-based hybrid models is better than the BPNN based ones because the sample data used for the rate constant regression model is too small, so the performance of BPNN is not fully shown. Thus, SVR is a better choice in the case of small experimental data when one wants to develop a hybrid model for the chemical process.

Finally, The SVR+Wang based hybrid model was chosen as the best suitable hybrid model for PX oxidation process according to the comparative study.

ACKNOWLEDGEMENTS

The authors gratefully acknowledge the support from the following foundations: 973 project of China (2013CB733605), National Natural Science Foundation of China (21176073) and the Fundamental Research Funds for the Central Universities.

NOMENCLATURE

C : cost function of support vector regression [-]
C_i : concentration of ith component in the p-xylene oxidation [mol/kg$_{HAc}$]
$C_{[O]_i}$: concentration of ith peroxy radicals [mol/kg$_{HAc}$]
d_i : kinetic parameters in the model of Wang [kg$_{HAc}$/mol]
k_i^{cao} : kinetic rate constant of the ith lumped reaction in the model of Cao [min^{-1}]
k_i^{wang} : kinetic rate constant of the ith lumped reaction in the model of Wang [min^{-1}]
k_i^{sun} : kinetic rate constant of the ith lumped reaction in the model of Sun [min^{-1}]
m_i : reaction order of two reactants of the ith lumped reaction [-]
n_i : reaction orders of two reactants of the ith lumped reaction [-]
N : number of experimental data [-]
r_i : reaction rate of the ith lumped reaction [mol/(kg$_{HAc}$·min)]
t : residence time [min]
x_1 : reaction temperature [°C]
x_2 : initial concentration of p-xylene [mol/kg$_{HAc}$]
x_3 : concentration of cobalt catalyst in the feed [ppmw]
x_4 : concentration of manganese catalyst in the feed [ppmw]
x_5 : concentration of bromide promoter in the feed [ppmw]
y_{exp} : experimental measurement value [mol/kg$_{HAc}$]
$y_{exp\,(mean)}$: mean value of experimental data [mol/kg$_{HAc}$]
y_{pred} : model prediction value [mol/kg$_{HAc}$]
$y_{pred\,(mean)}$: mean value of model prediction value [mol/kg$_{HAc}$]

Greek Letters

θ : kinetic parameters in the model of Wang [-]
β_i : kinetic parameters in the model of Wang [-]
σ : width of RBF kernel [-]
ε : loss function [-]

REFERENCES

1. J. H. Lee, S. B. Kim, H. Y. Yoo, J. H. Lee, C. Park, S. O. Han and S. W. Kim, *Korean J. Chem. Eng.*, **30**(6), 1272 (2013).
2. B. Duarte, P. Saraiva and C. Pantelides, *Int. J. Chem. React. Eng.*, **2**(1) (2004), DOI:10.2202/1542-6580.1128.
3. N. Patil, P. Shelokar, V. Jayaraman and B. Kulkarni, *Chem. Eng. Res. Des.*, **83**(8), 1030 (2005).
4. S. S. Haykin, *Neural networks: A comprehensive foundation*, Prentice-Hall Englewood Cliffs, NJ (2007).
5. S. Nandi, S. Ghosh, S. S. Tambe and B. D. Kulkarni, *AIChE J.*, **47**(1), 126 (2001).
6. M. Lashkarbolooki, A. Z. Hezave and A. Babapoor, *Korean J. Chem. Eng.*, **30**(1), 213 (2013).
7. T. C. Park, U. S. Kim, L.-H. Kim, B. W. Jo and Y. K. Yeo, *Korean J. Chem. Eng.*, **27**(4), 1063 (2010).
8. A. B. Gandhi, P. P. Gupta, J. B. Joshi, V. K. Jayaraman and B. D. Kulkarni, *Ind. Eng. Chem. Res.*, **48**(9), 4216 (2009).

9. V. Vapnik, *The nature of statistical learning theory*, Springer (1999).
10. S. K. Lahiri and K. C. Ghanta, *Korean J. Chem. Eng.*, **26**(5), 1175 (2009).
11. T. C. Park, T. Y. Kim and Y. K. Yeo, *Korean J. Chem. Eng.*, **27**(6), 1662 (2010).
12. C. J. Lee, J. W. Ko and G. Lee, *Korean J. Chem. Eng.*, **29**(2), 145 (2012).
13. A. Fazlali, P. Koranian, R. Beigzadeh and M. Rahimi, *Korean J. Chem. Eng.*, **30**(9), 1681 (2013).
14. D. E. Lee, S.-O. Song and E. S. Yoon, *Korean J. Chem. Eng.*, **21**(6), 1103 (2004).
15. D. C. Psichogios and L. H. Ungar, *AIChE J.*, **38**(10), 1499 (1992).
16. H. Qi, X.-G. Zhou, L.-H. Liu and W.-K. Yuan, *Chem. Eng. Sci.*, **54**(13), 2521 (1999).
17. G. Zahedi, A. Elkamel, A. Lohi, A. Jahanmiri and M. Rahimpor, *Chem. Eng. J.*, **115**(1), 113 (2005).
18. X. Yan, *Chem. Eng. Sci.*, **62**(10), 2641 (2007).
19. L. L. Simon, U. Fischer and K. Hungerbühler, *Ind. Eng. Chem. Res.*, **45**(21), 7336 (2006).
20. S. Ou and L. E. Achenie, *J. Power Sources*, **140**(2), 319 (2005).
21. B. Shiva Kumar and C. Venkateswarlu, *Bioresour. Technol.*, **103**(1), 300 (2012).
22. H. J. Zander, R. Dittmeyer and J. Wagenhuber, *Chem. Eng. Technol.*, **22**(7), 571 (1999).
23. G. Zahedi, A. Lohi and K. Mahdi, *Fuel Process. Technol.*, **92**(9), 1725 (2011).
24. Q. Sun, C. Pan and X. Yan, *Korean J. Chem. Eng.*, **30**(3), 518 (2013).
25. N. Luo, W. Du, Z. Ye and F. Qian, *Ind. Eng. Chem. Res.*, **51**(19), 6926 (2012).
26. H. Ince and T. B. Trafalis, *Decision Support Systems*, **42**(2), 1054 (2006).
27. B. P. Duarte and P. M. Saraiva, *Ind. Eng. Chem. Res.*, **42**(1), 99 (2003).
28. X. Wang, J. Chen, C. Liu and F. Pan, *Chem. Eng. Res. Des.*, **88**(4), 415 (2010).
29. R.-d. Jia, Z.-z. Mao, Y.-q. Chang and L.-p. Zhao, *Chem. Eng. Res. Des.*, **89**(6), 722 (2011).
30. G. Cao, M. Pisu and M. Morbidelli, *Chem. Eng. Sci.*, **49**(24), 5775 (1994).
31. Q. Wang, X. Li, L. Wang, Y. Cheng and G. Xie, *Ind. Eng. Chem. Res.*, **44**(2), 261 (2005).
32. W. Sun, Y. Pan, L. Zhao and X. Zhou, *Chem. Eng. Technol.*, **31**(10), 1402 (2008).
33. X. Yan and W. Zhao, *Intell. Autom. Soft. Co.*, **15**(1), 41 (2009).
34. Y. Xuefeng, *Chemometr. Intell. Lab.*, **103**(2), 152 (2010).
35. G. Cao, A. Servida, M. Pisu and M. Morbidelli, *AIChE J.*, **40**(7), 1156 (1994).
36. A. Cincotti, R. Orru, A. Broi and G. Cao, *Chem. Eng. Sci.*, **52**(21), 4205 (1997).
37. A. Cincotti, R. Orru and G. Cao, *Catal. Today*, **52**(2-3), 331 (1999).
38. X. Yan, W. Du and F. Qian, *AIChE J.*, **50**(6), 1169 (2004).
39. Q. Wang, Y. Cheng, L. Wang and X. Li, *Ind. Eng. Chem. Res.*, **46**(26), 8980 (2007).
40. Q. Wang, X. Li, L. Wang, Y. Cheng and G. Xie, *Ind. Eng. Chem. Res.*, **44**(13), 4518 (2005).
41. F. Qian, L. Tao, W. Sun and W. Du, *Ind. Eng. Chem. Res.*, **51**(8), 3229 (2012).
42. Y. Dong and X. Yan, *Ind. Eng. Chem. Res.*, **52**(7), 2537 (2013).
43. P. Raghavendrachar and S. Ramachandran, *Ind. Eng. Chem. Res.*, **31**(2), 453 (1992).
44. C. H. Bamford, *Comprehensive chemical kinetics*, Elsevier Science Ltd. (1972).
45. C. C. Chang and C. J. Lin, *ACM Transactions on Intelligent Systems and Technology (TIST)*, **2**(3), 27 (2011).